Influence of Pb(II) Ions on the EPR Properties of the Semiquinone Radicals of Humic Acids and Model Compounds: High Field EPR and Relativistic DFT Studies

Maciej Witwicki,*,† Maria Jerzykiewicz,† Adrian R. Jaszewski,† Julia Jezierska,† and Andrzej Ozarowski‡

Faculty of Chemistry, Wroclaw University, 14 F. Joliot-Curie Street, Wroclaw 50-283, Poland, and National High Magnetic Field Laboratory, Florida State University, 1800 East Paul Dirac Drive, Tallahassee, Florida 32310

Received: July 3, 2009; Revised Manuscript Received: November 4, 2009

X-band (9.76 GHz) and high field (416.00 GHz) electron paramagnetic resonance spectroscopy (EPR) was used to study the interactions between Pb(II) ions and semiquinone radicals of natural humic acids and their simple models. The EPR experiments were performed on powder samples. The formation of Pb(II) complexes with the radicals was accompanied by a significant decrease of *g* parameters as compared to those observed for parent radicals. Two types of complexes were identified depending on the initial concentration of Pb(II) ions. For one of them the anisotropic hyperfine coupling with the ^{207}Pb nucleus was observed. Systematic DFT calculations were carried out for complexes with different forms of radical ligands ($L_2^{-\bullet}$, $HL^{-\bullet}$, and $H_2L^{\bullet}$) derived from 3,4-dihydroxybenzoic acid representing different ligation schemes. The *g* parameters calculated for the structure characterized by a significant accumulation of spin density on the Pb atom are strongly deviated from the values observed experimentally. Moreover, a decrease of the spin population on all oxygen atoms as a result of complexation of Pb(II) via carboxyl oxygens and protonation of hydroxyl oxygens is required to reproduce the experimental *g* parameters.

1. Introduction

Humic substances (HSs) are the most widespread nonliving natural organic matter in terrestrial environment as well as in freshwater and seawater,[1–3] participating in the global carbon cycle and being responsible for many important properties of soils. HSs consist of various chemical compounds which can be divided into several fractions based on solubility in acids and alkalis.[1,2] The most important are (1) humin, insoluble in acidic and alkaline pH; (2) humic acids (HAs), soluble in alkaline water solutions and insoluble in acids; and (3) fulvic acids, soluble in both alkalis and acids.

HAs are dark brown or black fractions being a mixture of transformed biomolecules; thus, no crystal structure and no unique molecular formula of HAs or of any other HSs fractions is available. Nevertheless, a general model structure of HAs has been established based on analytical and spectroscopic analysis.[1,2] Humic acids exhibit supramolecular structures consisting of several major functional groups, mostly carboxylic and phenolic, along with carbonyl, quinonoid, and alcoholic. The phenolic and carboxyl groups of HAs are known to act as binding sites for metal ions,[3] for example, for Mg^{2+}, Cu^{2+}, Ca^{2+}, Zn^{2+}, Cd^{2+}, or Pb^{2+}.

Since the 1960s[4,5] electron paramagnetic resonance spectroscopy (EPR) has been used to investigate properties and chemistry of humic acids as stable organic free radicals are indispensable components of their structure.[2,6] Two types of the radicals in HAs are generally recognized: stable (*native*) and short-lived (*transient*).[2,6] The EPR studies showed a characteristic difference in the *g* values of these two types of radicals. Increasing pH from weak acidic to alkaline[2,6–9] or treatment of the solid humic acid by gaseous ammonia[10,11] causes the transformation of native radicals into the transient ones and the generation of additional transient systems, as evidenced by *g* parameter increase of 400−1000 ppm. Recently, high field EPR studies revealed the perpendicular and parallel **g** tensor components for both types of radicals.[9] Our DFT calculations for the model compound (3,4-dihydroxybenzoic acid, **34dhb**) allowed us to assign the protonated and deprotonated semiquinone forms to the stable and short-lived radicals, respectively.[12,13]

The concentration of organic free radicals in HAs and their *g* parameter values derived from the EPR spectra have been associated with the structure and reactivity of HA, and they are an important indication of the humification degree.[6,14–18] Moreover, significant changes in the free radicals concentration resulting from the interaction of HAs with metal ions were observed,[10,11,19,20] e.g., with Mg^{2+}, Cu^{2+}, Ca^{2+}, Zn^{2+}, or Cd^{2+}. This is particularly important as HAs together with clays and metal oxides are a key factor determining the metal binding in soils.[3] However, a completely different effect is observed for Pb^{2+} ions. The complexation of Pb^{2+} with humic acids macromolecules leads to formation of a new kind of stable radical species characterized by unusually low *g* values (∼2.001).[7,21]

Given the complicated and unresolved structure of humic acids, the model compounds of low molecular weight were used to mimic HAs as ligands. Hydroxy derivatives of benzoic acids and their esters were investigated to determine the factors allowing for formation of new radicals and to establish molecular and electronic structure of the system exhibiting the decrease of *g* parameters in the presence of Pb^{2+} ions.[7] The choice of model compounds was dictated by the widely accepted "polyphenol theory"[1–3] for the humic substance formation. According to this theory the major building blocks of HAs are polyphenols derived from lignin or synthesized by microorganisms. In this

* To whom correspondence should be addressed. E-mail: mck@eto.wchuwr.pl. Telephone: +48 (0)71 37 57 322. Fax: +48 (0)71 32 82 348.
† Wroclaw University.
‡ Florida State University.

10.1021/jp906289d
Published on Web 11/23/2009

model *p*-hydroxybenzoic acid, **34dhb**, and gallic acid (3,4,5-trihydroxybenzoic acid, **345thb**) are among the major low molecular weight precursors of HAs formed after lignin degradation. As reported previously, only dihydroxybenzoic acids with at least two *vicinal* hydroxyl groups are able to form the radicals characterized by very low *g* values in the presence of Pb^{2+} ions, and thus the structural units of HAs responsible for the radical formation have been identified.[7] It is also important that the radicals formed from model compounds are stable, similarly to the radicals derived from HAs.

Previous DFT calculations for model complexes of Pb(II) ion with trinegative radical of **345thb** revealed that spin density could be significantly delocalized onto the Pb atom when the complexation takes place via a carboxyl group.[7] This important conclusion was postulated to be a main reason for the observed *g* value lowering, which was to a certain degree supported by the FTIR spectroscopy, indicating interactions between Pb(II) ions and HAs via carboxyl groups.[21] However, no theoretical prediction of *g* parameter was done to back up this hypothesis. Recently, the UV and DFT studies on the complexation of Pb(II) with caffeic acid suggested that the carboxy moieties are the binding sites in weakly acidic conditions, when the hydroxyl groups are protonated.[22,23] Therefore, it should be noted that formation of Pb(II)-induced radicals from model compounds occurs as well under weakly acidic conditions.

In this work we decided to investigate in detail the interaction of Pb(II) ions with humic acids and their model compounds. X-band (9.6 GHz) and high field EPR (416.00 GHz) spectroscopies were applied, as valuable information about an interaction of *o*-semiquinones with metal ions can be extracted from the EPR studies.[24–29] Systematic DFT study of the model complexes between Pb(II) ions and semiquinone radicals was performed, in that various possible forms of radical ligand ($L_2^{-\bullet}$, $HL^{-\bullet}$, and $H_2L^{\bullet}$) were examined, and different kinds of possible metal cation binding schemes affecting the **g** tensor were considered. We have expected that the agreement between the theoretically predicted and experimentally obtained **g** tensors would reveal the structural types responsible for the low *g* values observed by the EPR spectroscopy, allowing for characterization of the best model mimicking the Pb(II) coordination to HA, which is an important problem for environmental chemistry.[3,30]

2. Experimental and Computational Approach

34dhb and **345thb** acids were purchased from Aldrich. Humic acids were extracted from peat ($\mathbf{HA_P}$) of Odra river lowland near Wroclaw (Lower Silesia, Poland) and from compost ($\mathbf{HA_C}$) derived from the Municipal Composting Plant in Zabrze (Upper Silesia, Poland). The isolation was carried out using standard International Humic Substances Society (IHSS) procedure.[1,2] To obtain the complexes of Pb(II) ions with $\mathbf{HA_C}$, $\mathbf{HA_P}$, **34dhb**, and **345thb** in powder form, a constant amount of a solid ligand (1 mmol of **34dhb** and **345thb** or 50 mg of $\mathbf{HA_C}$ and $\mathbf{HA_P}$) was treated with a fixed volume of lead acetate solution (20 mL) of concentration appropriate to obtain various initial Pb(II):*L* molar ratios from 1:1 to 5:1, where *L* = **34dhb** or **345thb**, and stirred for about 12 h. The pH of the reaction mixture was found to be in the range 4.90−5.30 for model compounds (pH was not adjusted by a buffer solution). The solid product was filtered and dried at room temperature, and the EPR spectra of powder samples were recorded.

For model compounds two types of complexes were identified depending on the initial content of Pb(II) ions in the reaction mixture: complex **1** derived from molar ratio Pb(II):*L* = 3:1 and complex **2** from molar ratio Pb(II):*L* = 2:1. These ratios were found to give optimal concentration of paramagnetic complexes.

X-band EPR (9.6 GHz) spectra were recorded at the room temperature on a Bruker ESP 300E spectrometer equipped with a Bruker NMR gauss meter ER 035 M and a Hewlett-Packard microwave frequency counter HP 5350B. The high field (416.00 GHz) EPR spectra were recorded at 10 K using the NHMFL high magnetic field facility.[31]

According to the spin-Hamiltonian formalism, the **g** tensor characterizes the interaction between the effective spin of the paramagnetic molecule **S** and the external magnetic field **B**. The appropriate electronic Zeeman term $\mathbf{H}^Z$ in atomic units may be written as

$$\mathbf{H}^Z = \frac{1}{2c}\cdot\mathbf{B}\cdot\mathbf{g}\cdot\mathbf{S} \tag{1}$$

It is convenient to consider the **g** tensor as a sum of the isotropic free electron g_e and a 3 × 3 matrix $\Delta\mathbf{g}$, which contains spin−orbit coupling and other relevant contributions

$$g = g_e\mathbf{I}_3 + \Delta\mathbf{g} \tag{2}$$

where $\mathbf{I}_3$ is the 3 × 3 unit matrix and $g_e = 2.002\ 319\ 30(...)$.[50] Because of the small EPR energy scale, the magnetic field dependent terms are best calculated as a perturbation. In the presence of spin−orbit coupling (SOC), the situation is more complex. For the light nuclei, SOC is weak and the perturbation treatment is justifiable. However, starting from the 5d transition metals, this approach becomes uncertain. Therefore, two distinct methods were developed. In the two-component methods, (1) SOC is treated variationally with the **g** tensor calculated as a first derivative of the energy. In the one-component approach, (2) the magnetic field and SOC are treated as perturbations and the **g** tensor becomes a second-order property. Full theoretical background for one-component[32–34] and two-component[33,35] approaches to the **g** tensor calculations is well described in the literature.

Because the systems investigated here contain lead, all single-point calculations of the **g** tensor were performed according to the two-component approach using the relativistic formalism ZORA for the spin−orbit coupling,[36] as implemented by van Lenthe[35] et al. in Amsterdam Density Functional[37] (ADF) version 2007.01. Three different functionals were used: (a) local density approximation of Vosko, Wilk, and Nusair[38] (VWN) with the exchange gradient correction proposed by Becke[39] (B) and the correlation term developed by Perdew[40] (P86); (b) VWN local density approximation with the exchange gradient correction and the correlation term by Perdew and Wang[41] (PW91); (c) B exchange gradient correction and the correlation term by Lee, Yang, and Parr[42] (LYP), which already contains the local correlation part. Standard all-electron Slater-type triple-ζ basis set plus polarization quality (TZP) was used for all atoms. The **g** tensor calculations were performed in the spin-unrestricted collinear approximation[43] that takes the spin polarization effects into account.

Since no crystal structures are available, the geometry optimizations were carried out with the ADF program package employing VWN local density approximation, B exchange gradient correction, and P86 correlation term combined with the standard all-electron Slater-type TZP basis set. No symmetry constraints were set in the geometry optimization procedures. Optimizations were performed within the unrestricted scalar ZORA relativistic formalism.[44] Each stationary point was fully characterized as a true minimum by the vibrational analysis.

TABLE 1: *g* Values and Hyperfine Constants *a* (in Gauss) for Humic Acids and Model Compounds[a]

34dhb	g_x	2.0062	$a^a_{iso}(^1H)$	3.30
	g_y	2.0057	$a^b_{iso}(^1H)$	1.38
	g_z	2.0026	$a^c_{iso}(^1H)$	0.76
	g_{iso}	2.0048		
34dhb complex **1**[b]	g_x	2.0046	$a_x(^{207}Pb)$	–
	g_y	2.0016	$a_y(^{207}Pb)$	–
	g_z	2.0016	$a_z(^{207}Pb)$	–
	g_{iso}	2.0026	$a_{iso}(^{207}Pb)$	–
	g_{eff}	2.0012		
34dhb complex **2**[b]	g_x	2.0065	$a_x(^{207}Pb)$	71.6
	g_y	2.0028	$a_y(^{207}Pb)$	–
	g_z	2.0008	$a_z(^{207}Pb)$	–
	g_{iso}	2.0034	$a_{iso}(^{207}Pb)$	–
	g_{eff}	2.0017		–
345thb	g_{iso}	2.0048	$a_{iso}(^1H)$	0.85
345thb complex **1**[b]	g_{eff}	2.0010	$a(^{207}Pb)$	–
345thb complex **2**[c]	g_{eff}	2.0013	$a_x(^{207}Pb)$	97.6
$\mathbf{HA_C}$	g_{eff}	2.0033		
$\mathbf{HA_P}$	g_{eff}	2.0036		
$\mathbf{HA_C}$ complex	g_{eff}	2.0012	$a(^{207}Pb)$	–
$\mathbf{HA_P}$ complex	g_{eff}	2.0013	$a(^{207}Pb)$	–

[a] g_{eff} was derived from the X-band (9.6 GHz) EPR spectra, the g_{iso} of **34dhb**, **34dhb** complex **1,** and **34dhb** complex **2** were obtained as the average of three components of the **g** tensor resolved in the high field EPR (416.00 GHz) spectra. All anisotropic hyperfine constants were determined from X-band spectra and were assigned as the *x*-component based on the high field EPR spectra. [b] Initial Pb(II):*L* molar ratio of 3:1. [c] Initial Pb(II):*L* molar ratio of 2:1.

3. Results and Discussion

3.1. Formation of Low *g* Radicals upon the Pb(II) Interaction. For all systems studied in this work, the effect of the Pb(II):*L* molar ratio was explored as described below. Since HAs are not a single chemical entity, the constant amount of particular HAs was treated with various amounts of Pb(II) ions. All *g* parameters and hyperfine constants derived from the X-band and high field EPR spectra are summarized in Table 1.

The radicals present in HAs reveal the *g* values varying from 2.0025 to 2.0045,[2,6] and, as it has been mentioned above, *g* is dependent strongly on the pH value.[6–11] The g_{eff} parameters observed for powder $\mathbf{HA_C}$ (2.0033) and $\mathbf{HA_P}$ (2.0036) are typical for humic acids. The *g* parameters observed for the powder Pb(II)−radical complexes obtained by mixing of Pb(II) acetate and **34dhb** or **345thb** are compared to those derived for the radicals generated from **34dhb** or **345thb** in ambient oxygen and alkaline water solution. Isotropic spectra of **34dhb** and **345thb** radicals were recorded in aqueous solutions at room temperature and anisotropic **34dhb** spectrum in frozen aqueous solution at 10 K.

The X-band isotropic EPR spectrum of **34dhb** radical anion exhibits the hyperfine splitting due to three nonequivalent protons of benzoic ring (g_{iso} = 2.0048, $a(^1H)_{iso}{}^a$ = 3.30 G, $a(^1H)_{iso}{}^b$ = 1.38 G, and $a(^1H)_{iso}{}^c$ = 0.76 G), while splitting from two equivalent protons (g_{iso}= 2.0048, $a(^1H)_{iso}$ = 0.85 G) is observed for **345thb**.

Treatment of solid $\mathbf{HA_C}$ and $\mathbf{HA_P}$ with lead acetate solution results in a characteristic modification of the EPR signal. Total signal intensity increases as compared to that recorded for the pure HAs. The native radical concentration in the $\mathbf{HA_C}$ was found to be about 0.3×10^{18} spins per gram. After formation of Pb(II)−$\mathbf{HA_C}$ complex the concentration increases even to 1.7×10^{18} spins per gram. Subtraction of the HAs signal from the signal of Pb-treated HAs reveals a new radical line (see Figure 1), as reported previously.[7] The *g* values for new radicals

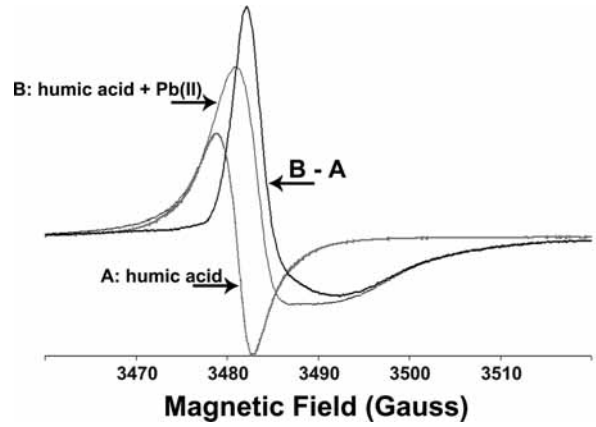

Figure 1. Room-temperature X-band (9.6 GHz) EPR spectra of $\mathbf{HA_c}$ powder (trace A), Pb-treated $\mathbf{HA_c}$ powder (trace B), and numerical subtraction of A from B.

in both Pb−HAs systems are significantly smaller than those for native radicals that occur in HAs: g_{eff} = 2.0012 for Pb−$\mathbf{HA_C}$ compared to g_{eff} = 2.0033 for $\mathbf{HA_C}$ and 2.0013 for Pb−$\mathbf{HA_P}$ compared to 2.0036 for $\mathbf{HA_P}$. Nevertheless, no significant dependence of EPR parameters on concentration of Pb(II) was observed. The high field EPR spectra of powdered HAs and Pb−HAs systems did not reveal the **g** tensor components.

It needs to be noticed that the presence of indigenous signal due to HAs in the spectra of Pb(II)-treated HAs proves that the native radicals, which are probably located in the humic acid macromolecular matrix, are not affected by the Pb(II) ions. Pb(II) seems to be bonded mainly to the outer macromolecular fragments. Furthermore, if the Pb(II) ions were involved in the interaction with the native radical sites in HAs giving the $g \sim 2.001$ signals, the complexes could not be generated from model dihydroxybenzoic acids (since dihydroxybenzoic acids do not contain the native radicals). Therefore, it can be assumed that the radical complexes formation is preceded by the Pb(II) ions coordination to the diamagnetic ligand.

In contrast to HAs, the initial concentration of Pb(II) ions appeared to be a major factor determining the EPR parameters observed for radical complexes with **34dhb** and **345thb** ligands. Two types of spectra were observed depending on Pb(II) concentration (see Figure 2). For the system prepared using molar ratio Pb(II):*L* = 3:1, the powder EPR spectra indicating formation of complex **1** are similar to those reported previously ($g_{eff} \sim 2.001$).[7] However, the spectra of the Pb(II):*L* = 2:1 system differ distinctly from those observed when molar ratio Pb(II):*L* = 3:1 was used. They are stronger and slightly anisotropic, with larger g_{eff}, but still below the g_{iso} values for the radical anions derived from the parent hydroxybenzoic acids. In addition, the powder EPR spectra for the 2:1 system show satellite splitting due to the anisotropic hyperfine interaction of an unpaired electron with the ^{207}Pb nucleus (I = 1/2, 22.1% abundance). Therefore, the second complex (complex **2**) has been identified. Its high field EPR spectrum reveals three **g** tensor components (Figure 3, spectrum B): g_x is slightly higher than that for radical anion derived from **34dhb**, while g_y and g_z are significantly reduced. These parameters and hyperfine couplings with the ^{207}Pb nucleus strongly suggest a covalent interaction between the Pb(II) ion and a radical ligand in complex **2**. $a_x(^{207}Pb)$ is larger and g_{eff} is lower for the complex **2** of **345thb** than for the complex **2** of **34dhb**. This suggests that even small changes in the spin population on the Pb atom can lead to a significant change of the experimental EPR parameters.

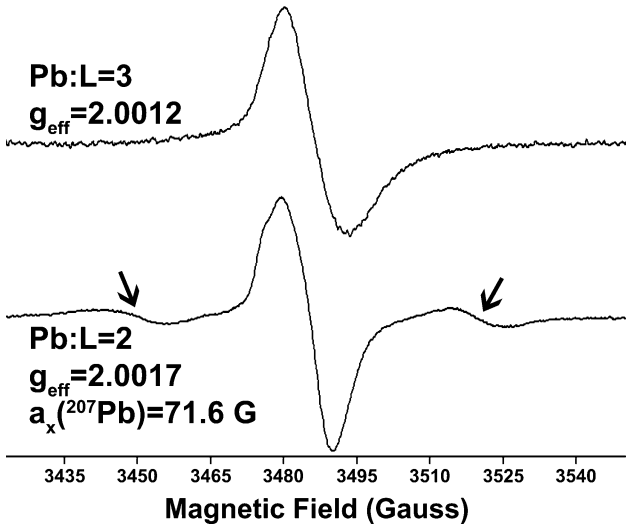

Figure 2. Room-temperature X-band (9.6 GHz) EPR spectra of powders of Pb(II)−radical complexes formed in the **34dhb**−Pb(II) system with two different molar Pb(II):*L* ratios. The arrows point at the hyperfine lines due to the ^{207}Pb nucleus (I = 1/2, 22.1% abundance).

The high field EPR signal recorded for the Pb:*L* = 3:1 system (see spectrum C in Figure 3) is weaker than that observed for complex **2**, and new **g** tensor parameters (g_x = 2.0046, g_y = 2.0016, g_z = 2.0016) prove the formation of Pb(II) complex **1**.

The hyperfine constant, $a_x(^{207}Pb)$ = 71.6 G, is close to a_{iso} determined for the Pb(II) complexes with semiquinones derived from 3,5-di-*tert*-butyl-*o*-benzoquione and phenanthrenequinone (∼53 G)[47] as well as 3,6-di-*tert*-butyl-*o*-benzoquinones (50−80 G).[48] However, the recording of the isotropic EPR spectrum in current studies was impossible because dissolving of the Pb(II) complexes is possible only in alkaline pH and results in a disappearance of the radical signal. The g_{iso} values of about 1.999[47,48] are observed for the Pb(II) complexes with di-*tert*-butyl-*o*-benzosemiquiones or phenanthrenesemiquinone that provide hydroxyl groups only. This is well below the values observed for complex **2** (g_{iso}= 2.0034) and complex **1** (g_{iso}=2.0026), and thus the coordination via hydroxyl oxygens in the systems under study here seems to be all the more questionable. Moreover, further decrease of the **g** tensor components for complex **1** suggests an additional delocalization of the spin density onto the Pb atom, probably as a result of weak interaction of the same ligand molecule with another Pb(II) ion, as implied by higher initial molar Pb(II):*L* ratio. However, the EPR spectra recorded for complex **1** do not show satellite splitting due to the hyperfine interaction of an unpaired electron with the ^{207}Pb nucleus. This can be explained by weaker EPR signal observed for complex **1** formed in the sample and simultaneously by a low natural abundance of ^{207}Pb. As a result the intensity of flanking signals for complex **1** can be too weak to be detected.

3.2. DFT Computations for Model Complexes of Pb(II) with Semiquinone Radical Species. Three different forms of ligand were considered: $L^{2-\bullet}$, $HL^{-\bullet}$, and $H_2L^{\bullet}$. The radical derived from **34dhb** is an ambidentate ligand, and many possible isomers exist for every form. Two binding sites (carboxylic or phenolic oxygens) were taken into account for the ligand acting as either mono- or bidentate. First, the geometry of the Pb(II):*L* 1:1 model complexes and their *g* parameters were calculated. Next, analogous calculations were performed for model 1:2 complexes that were derived from those 1:1 complexes in which a reasonable agreement between the theoretical and experimental

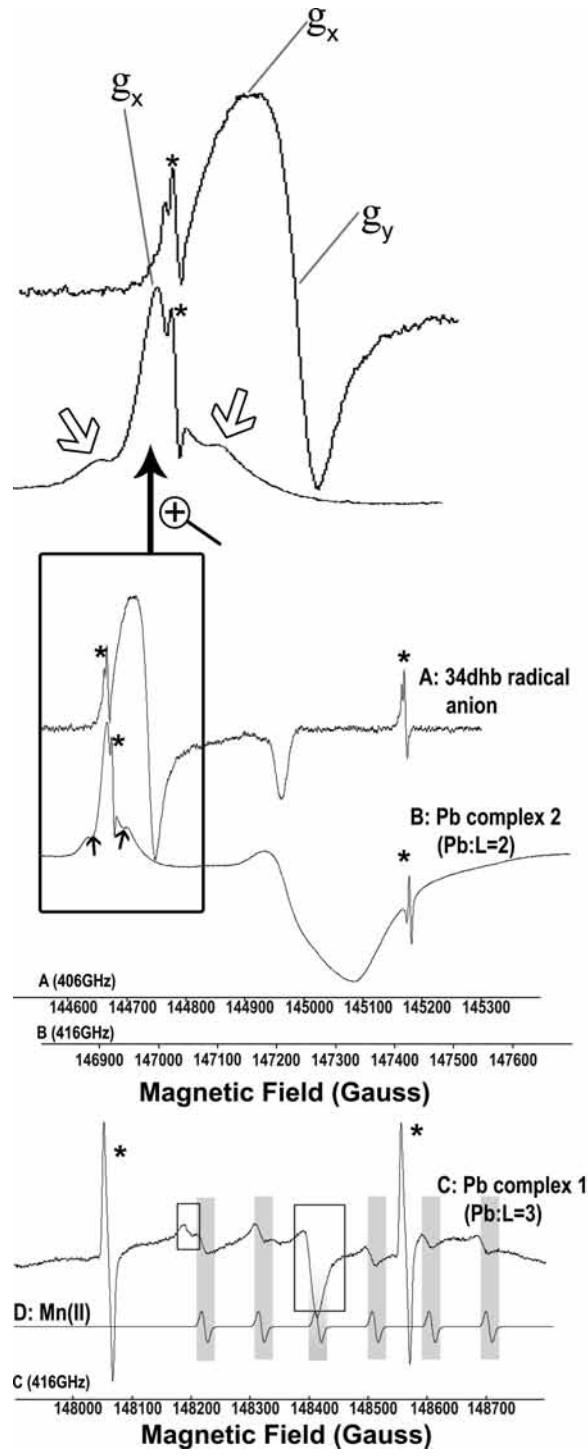

Figure 3. High field EPR spectra recorded at 10 K for the **34dhb** radical anion (spectrum A, frozen alkaline water solution) and for two types of **Pb(II)** powder complexes with radical ligand derived from **34dhb** (spectra B and C). Asterisks: signals of a standard (hydrogen atoms trapped in octaisobutylsilsesquioxane, g = 2.00294, A = 505.5 G[45,46]). Gray stripes indicate the hyperfine components due to the $^{55}Mn^{2+}$ contamination (simulated in trace D). Rectangles mark the signals of complex **1**. The arrows point toward the "perpendicular" hyperfine components due to the ^{207}Pb nucleus (I = 1/2, 22.1% abundance).

g tensors was achieved. All resulting structures are presented in Figures 4 and 5, and their structural parameters are summarized in the Supporting Information S.1.

For the discussion clarity, the 1:1 model complexes are divided into three groups ($[PbL]^{\bullet}$, $[Pb(HL)]^{+,\bullet}$, and $[Pb(H_2L)]^{2+,\bullet}$). The calculated structures in each group exhibit

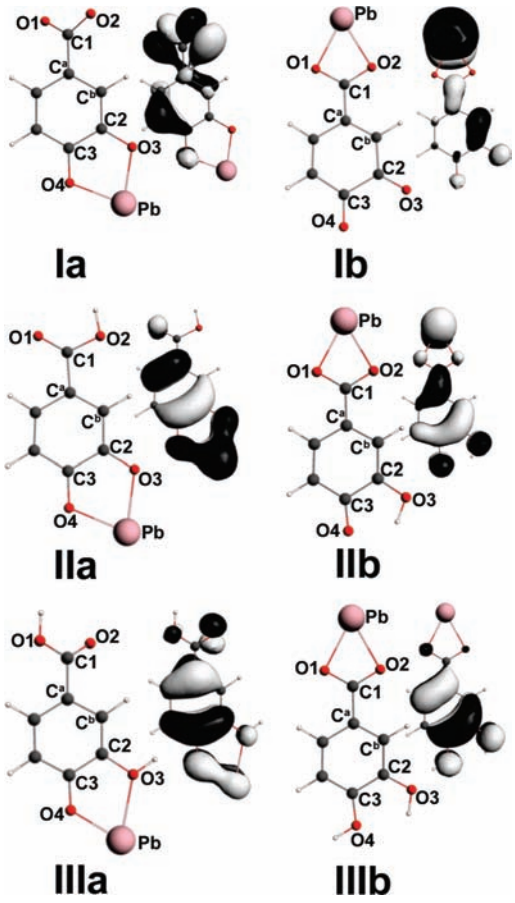

Figure 4. Structures of the 1:1 model complexes with the atoms numbering and singly occupied molecular orbitals (SOMOs) isosurfaces (0.03 au) predicted at the VWNBP86/TZP level.

two different binding modes, with either two oxygen donor atoms of carboxyl group (structures **Ib**, **IIb**, **IIIb**) or with two oxygen donor atoms of phenolic groups (structures **Ia**, **IIa**, **IIIa**). The isomers of the lowest ΔE^0 were chosen for the discussion, while the monodentate coordination modes were found to be energetically unfavorable.

Previously, only the complexes with fully deprotonated **345thb** radical anion were studied, and it was shown that the complexation of Pb(II) via carboxyl oxygens results in the delocalization of spin density onto the Pb atom.[7] This agrees with our DFT calculations. In Figure 4 the singly occupied molecular orbitals (SOMOs) are displayed, and the SOMO of **Ib** shows a large contribution from the Pb $6p_z$ orbital. For the **IIb** structure the accumulation of spin density on the Pb atom is also significant,; however, contributions from the O1, O2, O3, O4, and carbon atoms of benzoic ring are by far more important. In contrast, for the **IIIb** structure ($[PbH_2L]^{2+,\bullet}$) no significant Pb contribution to the SOMO is predicted. Furthermore, the general orbital shape and main contributions from the remaining atoms are very similar to the SOMO of radical anion derived from **34dhb**[12,13] (see Supporting Information S.2).

When the Pb(II) ion is coordinated to the hydroxyl oxygen atoms (**Ia**), a major accumulation of the spin density on the carboxyl oxygens (O2 and O3) is predicted due to a significant contribution of the $2p_x$ and $2p_y$ orbitals to the SOMO. Moreover, the Mulliken spin population on the lead atom is significant (see Table 2) and clearly indicates that Pb(II) participates in the radical character of the **Ia** model complex. Previously, a quite significant accumulation of spin density on the hydroxyl

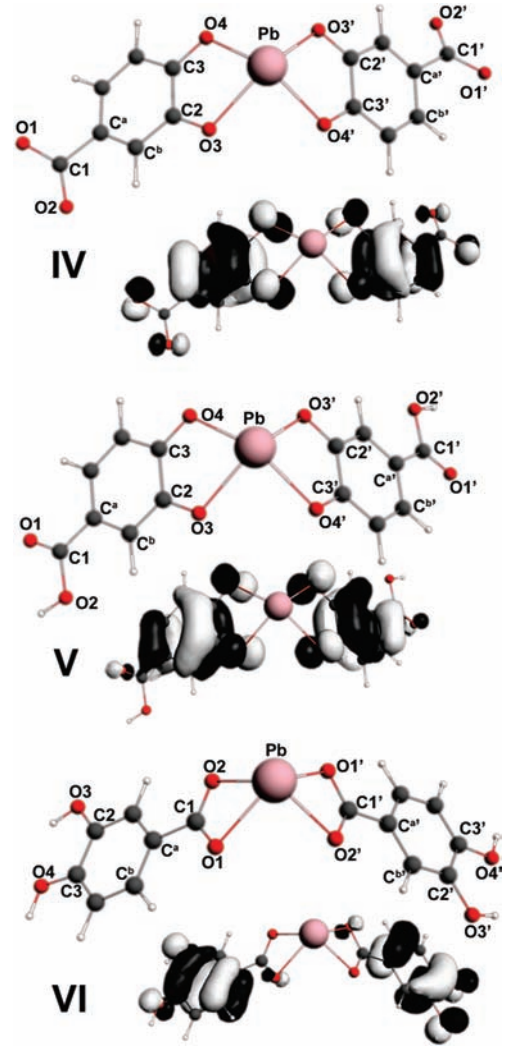

Figure 5. Structures of the 1:2 models with atoms numbering and SOMO isosurfaces (0.03 au) predicted at the VWNBP86/TZP level.

oxygen, not participating in bonding of Pb(II) ion, was predicted for the analogous complex with **345thb** radical.[7]

The SOMO predicted for the **IIa** structure reveals a distinct contribution from the $2p_z$ orbitals of ring carbon atoms and hydroxyl oxygen atoms (O3 and O4). However, a contribution from the Pb $6p_z$ orbital is significant and results in the large spin population on this atom (see Table 2).

For the **IIIa** structure the large contributions to the SOMO from the $2p_z$ orbitals of ring carbons are predicted, and contributions from the O3 $2p_z$ and Pb $6p_z$ orbitals are significantly lower than for **IIa**. As a result the spin populations on these atoms are reduced in comparison to those for **IIa**. Finally, an important contribution from the O2 $2p_x$ and $2p_z$ as well as a small one from the O1 $2p_z$ orbitals are predicted and indicate a significant accumulation of spin population on O2.

The calculated **g** tensors (Table 3) for both $[PbL]^{\bullet}$ complexes reveal that for the **Ib** structure, representing the complexation via carboxyl group, all computed values of **g** tensor are significantly underestimated. Therefore, a significant accumulation of spin population on the Pb atom, suggested previously, cannot be responsible for the experimentally observed *g* shift. Furthermore, the spin density accumulated on the carboxyl oxygens accompanied by the appreciable spin population on the Pb atom in the **Ia** structure also leads to the underestimation of **g** tensor. However, the **g** tensor components are closer to

TABLE 2: Mulliken Spin Populations Calculated at the VWNBP86/TZP Level

	$[PbL]^{\bullet}$		$[PbHL]^{+,\bullet}$		$[PbH_2L]^{2+,\bullet}$		$[PbL_2]^{3-,\bullet}$	$[Pb(HL)_2]^{-,\bullet}$	$[Pb(H_2L)_2]^{+,\bullet}$	$L^{2-,\bullet}$
	Ia	**Ib**	**IIa**	**IIb**	**IIIa**	**IIIb**	**IV**	**V**	**VI**	radical[a]
Pb[b]	0.060	0.716	0.146	0.175	0.054	0.005	0.003	−0.007	−0.001	−
O1	0.395	−0.022	0.049	0.015	0.292	0.018	0.044	0.019	0.015	0.023
O1′	−	−	−	−	−	−	0.046	0.019	0.015	−
O2	0.366	−0.026	−0.002	0.006	0.019	0.004	0.017	0.001	0.001	0.000
O2′	−	−	−	−	−	−	0.016	0.001	0.001	−
O3	0.003	0.104	0.108	0.115	0.019	0.190	0.083	0.127	0.090	0.232
O3′	−	−	−	−	−	−	0.085	0.127	0.090	−
O4	0.028	0.018	0.087	0.186	0.113	0.112	0.090	0.095	0.055	0.208
O4′	−	−	−	−	−	−	0.091	0.095	0.055	−
Σ(O)	0.792	0.074	0.242	0.322	0.443	0.324	0.475	0.477	0.321	0.463
Σ(C)	0.153	0.220	0.624	0.512	0.520	0.689	0.542	0.545	0.696	0.561

[a] Radical is the fully deprotonated **34dhb** radical anion ($L^{2-,\bullet}$). [b] Assuming that $a_{iso}(^{207}Pb) \approx (1/3)\, a_x(^{207}Pb)$ the experimental value of s-type spin population on the Pb atom was estimated to be ±0.0008.

TABLE 3: Theoretical and Experimental g Tensor Values

			g_x	g_y	g_z	g_{iso}
VWNBP86/TZP	$[PbL]^{\bullet}$	**Ia**	2.00144	1.98135	1.95956	1.98078
		Ib	1.64136	1.42227	1.12589	1.39651
	$[PbHL]^{+,\bullet}$	**IIa**	1.90335	1.83535	1.79555	1.84475
		IIb	1.91488	1.85712	1.80833	1.86011
	$[PbH_2L]^{2+,\bullet}$	**IIIa**	1.98367	1.95442	1.93821	1.95877
		IIIb	2.00238	2.00146	1.99832	2.00072
	$[PbL_2]^{3-,\bullet}$	**IV**	2.00720	1.99580	1.98270	1.99523
	$[Pb(HL)_2]^{-,\bullet}$	**V**	2.01110	2.00180	1.99900	2.00397
	$[Pb(H_2L)_2]^{+,\bullet}$	**VI**	2.00550	2.00360	2.00150	2.00353
	$L^{2-,\bullet}$	radical	2.00887	2.00730	2.00203	2.00607
VWNPW91/TZP	$[PbL_2]^{3-,\bullet}$	**IV**	2.00702	1.99573	1.98260	1.99512
	$[Pb(HL)_2]^{-,\bullet}$	**V**	2.01087	2.00141	1.99870	2.00366
	$[Pb(H_2L)_2]^{+,\bullet}$	**VI**	2.00551	2.00364	2.00152	2.00356
BLYP/TZP	$[PbL_2]^{3-,\bullet}$	**IV**	2.00686	1.99617	1.98203	1.99502
	$[Pb(HL)_2]^{-,\bullet}$	**V**	2.01070	2.00104	1.99871	2.00348
	$[Pb(H_2L)_2]^{+,\bullet}$	**VI**	2.00550	2.00359	2.00152	2.00354
BP86/EPR-II[a]	$L^{2-,\bullet}$	**radical**	2.00632	2.00584	2.00223	2.00480
experimental	$L^{2-,\bullet}$	**radical**	*2.0062*	*2.0057*	*2.0026*	*2.0048*
	−	*complex* ***1***	*2.0046*	*2.0016*	*2.0016*	*2.0026*
	−	*complex* ***2***	*2.0065*	*2.0028*	*2.0008*	*2.0034*

[a] Taken from our previous calculations.[13]

the experimental data than that derived for **Ib**, and the **Ia** structure is also energetically favorable by about 9.0 kcal/mol, as expected on the basis of higher stability of five- versus four-membered ring.

When the $[PbHL]^{+\bullet}$ complexes are considered, the predicted **g** tensors for **IIa** and **IIb** are considerably underestimated. In both structures a significant contribution from the Pb $6p_z$ orbital to the SOMO results in a strong delocalization of spin density onto the Pb atom, and it is a main reason for reduced **g** tensor components as compared to those predicted for the parent radical anion. The coordination of Pb(II) ion via the hydroxyl oxygens (**IIa**) is energetically favorable over **IIb** by about 12.6 kcal/mol, and the **g** tensor components are distinctly closer to the experimentally observed ones.

DFT calculations for the complexes with doubly protonated ligand ($[PbH_2L]^{2+\bullet}$) reveal that the coordination via hydroxyl oxygen atoms (**IIIa**) results in all **g** tensor components well below the experimentally observed ones, again due to the Pb $6p_z$ contribution to the SOMO leading to a substantial accumulation of spin population on the Pb atom. However, for **IIIa** this spin population is clearly lower than for **IIa**, and the **g** tensor component values increase. Those predicted for the **IIIb** structure turned out to be quite close to the *g* parameters determined from the high field EPR spectrum. Summarizing, the higher the spin population on the Pb atom, the lower the **g** tensor components. The calculations for **IIIb** predict the spin population migration from all oxygen atoms to the carbon atoms as compared to the **34dhb** radical anion. Moreover, the **IIIb** structure is also energetically favorable by 20.4 kcal/mol, because the hydroxyl oxygen protonation effect easily overcomes the gain in energy resulting from the five-membered ring formation. Thus, it may be concluded that the coordination mode of **34dhb** radical ligand employing carboxyl oxygen atoms and both hydroxyl oxygen atoms being protonated (**IIIb**) is the best model for the experimentally observed EPR properties of the Pb−HAs systems.

To confirm this hypothesis, the coordination number of Pb(II) ion in the next step of calculations was doubled for the **Ia**, **IIa**, and **IIIb** structures. The comparison of experimentally observed **g** tensors with those calculated for the 1:1 models as well as relative energy analysis allowed for the exclusion of **Ib**, **IIb**, and **IIIa** model complexes.

The **g** tensor prediction for the 1:2 models (see Table 3) clearly indicates that the Pb(II) coordination by the species with protonated hydroxyl oxygens via carboxyl oxygen atoms (**VI**) is indeed responsible for the experimentally observed magnitudes of the **g** tensor components in complex **2**. The values computed for **IV** and **V** do not correlate so favorably with the experimental parameters. For **IV**, only g_x is close to its experimental counterpart. In case of **V**, g_y and g_z are reasonably close to the suitable components; however, g_x is significantly overestimated. A general improvement in the predicted values for **V** is caused by a significant decrease of contribution from the Pb $6p_z$ orbital to the SOMO, while in case of **IV** it is caused by a decrease of contribution from the carboxyl oxygens $2p_x$ and $2p_y$ orbitals as well as by the spin population lowering on the Pb atom.

The spin populations predicted for **VI** are generally similar to those of **IIIb**, but they are equally delocalized onto both ligand molecules (see Table 2). The total spin populations on all oxygen and all carbon atoms as well as on the Pb atom differ only insignificantly from those obtained for **IIIb**. Nevertheless, in case of the Pb atom, whose spin−orbit coupling is very large, even small changes in the spin population can result in substantial changes in the **g** tensor.

Concluding, only the spin structures predicted for **IIIb** and **VI** properly reproduce the **g** tensor observed for the experimentally well characterized complex **2**. Therefore, the spin density delocalization from the hydroxyl oxygens onto the ring carbon atoms, but not the spin accumulation on the Pb atom, seems to be the reason for the observed lowering of **g** tensor magnitudes compared to the parent radical.

This conclusion is supported by two other experimental results. (1) For the Pb(II) complex with 3,5-di-*tert*-butyl-*o*-

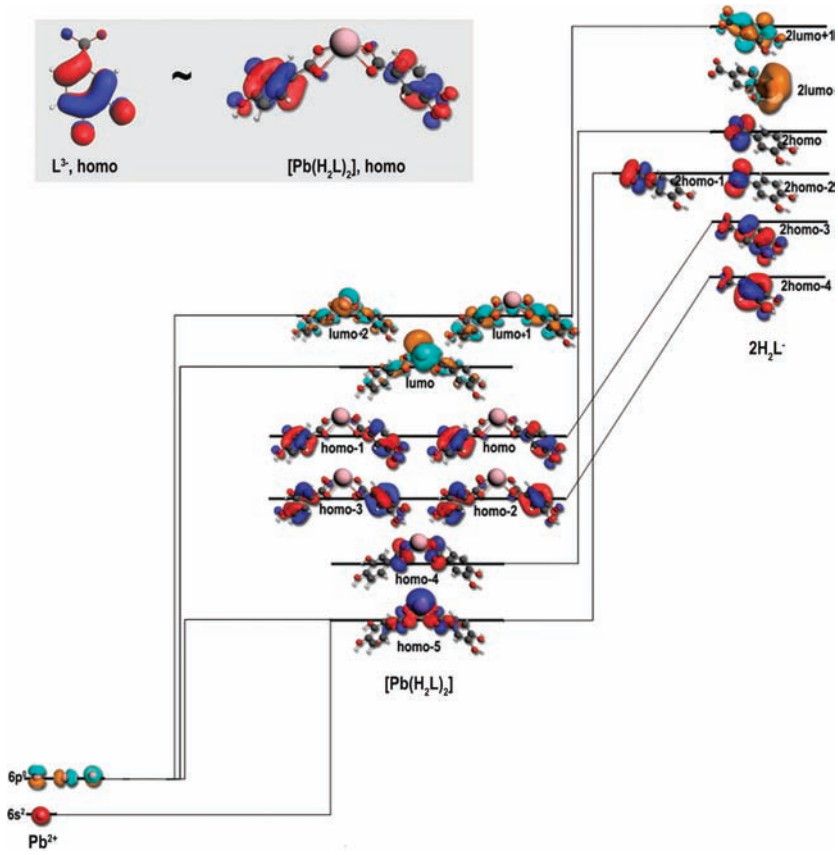

Figure 6. Orbital interaction diagram of two H_2L^- ligands and Pb(II) ion. The HOMOs of the trinegative **34dhb** anion (L^{3-}) and diamagnetic $[Pb(H_2L)_2]$ complex are compared in the gray rectangle.

benzosemiuione, g_{iso} was determined to be 1.9995[47] and 1.9998 for the complex with phenanthrenesemiquinone.[47] Those values are in accordance with the DFT predictions for the **IV** structure providing an additional argument against the coordination via hydroxyl oxygens in case of **34dhb** derivatives. (2) Furthermore, the studies on diamagnetic complexes of Pb(II) with caffeic acids revealed that the carboxy moieties are the binding sites while the hydroxyl groups are protonated,[22,23] thus supporting the structure proposed in this work.

The impact of the functional was found to be insignificant (see Table 3), since the differences between particular components of **g** tensor obtained from the calculations employing different functionals are negligible in context of the observed *g* shifts.

The perpendicular **g** tensor components calculated for the radical anion derived from **34dhb** are overestimated. To get accurate results the inclusion of the solvent molecules around a radical in the calculation is mandatory, as has been discussed previously.[13]

3.3. Reaction Mechanism. The DFT computations performed at the VWNBP86/TZP level for various radical ligand forms show that the radical species $\mathbf{R_1}$ arising from a homolytic scission of the carboxylic O−H group have significantly higher energies (at least 22 kcal/mol) than the $\mathbf{R_2}$ radical derived from a breaking of the O−H bond in the hydroxyl group. These data are in agreement with previous reports[12,49] and can be explained by lower resonance stabilization for $\mathbf{R_1}$, as the oxygens of carboxyl group are not involved in resonance with the benzoic ring. Thus, the participation of $\mathbf{R_1}$ radical in the reaction seems to be improbable, and the paramagnetic complex (**IIIb** or **VI**) cannot be formed by a direct coordination of Pb(II) ion to the $\mathbf{R_1}$ radical. Hence, it is more likely that a diamagnetic complex of the **34dhb** monoanions H_2L^- and Pb(II) is formed in the first step:

$$n\mathrm{H_2L^-} + \mathrm{Pb^{2+}} \rightarrow [\mathrm{Pb(H_2L)}_n]^{2-n} \quad (3)$$

In the second step the formation of paramagnetic complex occurs, possibly through oxidation by ambient O_2:

$$[\mathrm{Pb(H_2L)}_n]^{2-n} - \mathrm{e^-} \rightarrow [\mathrm{Pb(H_2L)}_n]^{3-n\cdot} \quad (4)$$

The formation of diamagnetic complex is schematically presented in Figure 6. The ligands HOMO, HOMO−1, and HOMO−2 are stabilized when interacting with the Pb(II) ion. Moreover, the HOMO−3 orbitals of two ligands become the degenerate HOMO and HOMO−1 of diamagnetic complex. The contributions of particular atoms to the diamagnetic complex HOMO orbital and the general orbital shape are very similar to those exhibited by the HOMO of the trinegative **34dhb** anion (see Figure 6), which is easily oxidized by ambient oxygen to its radical form. The chemical likeness of these orbitals may explain the propensity of diamagnetic complexes to oxidation that leads to open shell systems. However, an analogous orbital arrangement is predicted for the 2,5-dihydroxybenzoic acid (**25dhb**) complex as well (see Supporting Information S.3), but the latter one does not form radicals under treatment with Pb(II). Mixed coordination via one carboxyl and one hydroxyl oxygen can be excluded as a factor preventing the oxidation in case of **25dhb**, what is reasonable taking into account that 2,3-dihydroxybenzoic acid is known to form the Pb(II) radical complexes with low *g* values.[7] This implies that the vicinal hydroxyl groups may be required to form a transition state in the oxidation process.

4. Summary and Conclusions

X-band (9.6 GHz) and high field EPR (416.00 GHz) spectroscopy has been applied to investigate the radical complexes of Pb(II) ions with semiquinone radicals of HAs and their model compounds (**34dhb** and **345thb**). They exhibit unusually low *g* parameters compared to the parent radicals. For the model compounds, formation of two complexes (complex **1** and complex **2**) has been revealed by two different high field EPR spectra characterized by dissimilar patterns of the **g** tensor components. For complex **2**, the splitting due to anisotropic hyperfine interaction with the ^{207}Pb nucleus (I = 1/2, 22.1%) has been observed.

Systematic theoretical studies for the Pb(II)−**34dhb** system has shown that the structures with a significant accumulation of spin population on the Pb atom cannot explain the shifts of experimentally observed **g** tensor components. DFT investigations have indicated that only the decrease of spin population on all oxygen atoms accompanied by corresponding spin population increase on the carbon atoms of benzoic ring can reproduce the experimental results and most likely is responsible for the observed shifts of **g** tensor components. This was predicted for the structures with lead atom bonded via carboxyl oxygen atoms and with both hydroxyl oxygen atoms being protonated. Therefore, the binding mode and the form of ligands involved in the Pb−semiquinone complexes have been confirmed.

The reaction mechanism leading to the paramagnetic complex formation which includes two steps, formation of diamagnetic Pb(II) complex with **34dhb** and its oxidation into the radical form, has been proposed.

Acknowledgment. All computations were performed using computers of the Wrocław Center for Networking and Supercomputing (Grant No. 48). The high field EPR spectrum measurement was supported by NHMFL. The NHMFL is funded by the NSF through the Cooperative Agreement No. DMR-0654118, by the State of Florida, and by the DOE. This work was financially supported by MNiSW (Grant No. 2PO4G 06 30).

Supporting Information Available: The geometrical parameters of all optimized structures and further details of the DFT calculations. This material is available available free of charge via the Internet at http://pubs.acs.org.

References and Notes

(1) Stevenson, F. J. *Humus Chemistry. Genesis, Composition, Reactions*, 2nd ed.; John Wiley and Sons: New York, 1994.
(2) Senesi N.; Loffredo, E. In Sparks, E. D. *Soil Physical Chemistry*, 2nd ed.; CRC Press: Boca Raton, FL, 1999.
(3) Tipping, E. *Cation Binding by Humic Substances*, 1st ed.; Cambridge University Press: Cambridge, U.K., 2002.
(4) Rex, R. W. *Nature* **1960**, *188*, 1185.
(5) Steelink, C.; Tollin, G. *Biochim. Biophys. Acta* **1962**, *59*, 2534.
(6) Senesi, N. *Adv. Soil Sci.* **1990**, *14*, 77.
(7) Giannakopoulos, E.; Christoforidis, K. C.; Tsipis, A.; Jerzykiewicz, M.; Deligiannakis, Y. *J. Phys. Chem. A* **2005**, *109*, 2223.
(8) Paul, A.; Stosser, A. Z.; Zwirnmann, E.; Vogt, R. D.; Steinberg, C. E. *Environ. Sci. Technol.* **2006**, *40*, 5897.
(9) Christoforidis, K. C.; Un, S.; Deligiannakis, Y. *J. Phys. Chem. A* **2007**, *111*, 11860.
(10) Jezierski, A.; Czechowski, F.; Jerzykiewicz, M.; Chen, Y.; Drozd, J. *Spectrochim. Acta A* **2000**, *56*, 379.
(11) Jezierski, A.; Czechowski, F.; Jerzykiewicz, M.; Golonka, I.; Drozd, J.; Bylinska, E.; Chen, Y.; Seaward, M. R. D. *Spectrochim. Acta A* **2002**, *58*, 1293.
(12) Witwicki, M.; Jaszewski, A. R.; Jezerska, J.; Jerzykiewicz, M.; Jezierski, A. *Chem. Phys. Lett.* **2008**, *462*, 300.
(13) Witwicki, M.; Jezierska, J.; Ozarowski, A. *Chem. Phys. Lett.* **2009**, *473*, 160.
(14) Riffaldi, R.; Schnitzer, M. *Sci. Soc. Am. J.* **1972**, *36*, 301.
(15) Schnitzer, M.; Levesque, M. *Soil Sci.* **1979**, *127*, 140.
(16) Martin-Neto, L.; Nascimento, O. R.; Talamoni, J.; Poppi, N. R. *Soil Sci.* **1991**, *51*, 369.
(17) Barančiková, G.; Senesi, N.; Brunetti, G. *Geoderma* **1997**, *78*, 241.
(18) Jezierski, A.; Drozd, J.; Jerzykiewicz, M.; Chen, Y.; Kaye, K. J. *Appl. Magn. Reson.* **1998**, *14*, 275.
(19) Jerzykiewicz, M.; Drozd, J.; Jezierski, A. *Chemosphere* **1999**, *92*, 253.
(20) Jerzykiewicz, M.; Jezierski, A.; Czechowski, F.; Drozd, J. *Org. Geochem.* **2002**, *33*, 265.
(21) Jerzykiewicz, M. *Geoderma* **2004**, *122*, 305.
(22) Boilet, L.; Cornard, J.-P.; Lapouge, C. *J. Phys. Chem. A* **2005**, *109*, 1952.
(23) Cornard, J.-P.; Lapouge, C. *Chem. Phys. Lett.* **2007**, *438*, 41.
(24) Eaton, D. R. *Inorg. Chem.* **1964**, *3*, 1268.
(25) Felix, C. C.; Hyde, J. S.; Sarna, T.; Sealy, R. C. *J. Am. Chem. Soc.* **1978**, *100*, 3922.
(26) Felix, C. C.; Sealy, R. C. *J. Am. Chem. Soc.* **1982**, *104*, 1555.
(27) Kalyanaraman, B.; Felix, C. C.; Sealy, R. C. *Environ. Health Perspect.* **1985**, *64*, 185.
(28) Yuasa, J.; Suenobu, T.; Fukuzumi, S. *Chem. Phys. Chem.* **2006**, *7*, 942.
(29) Yuasa, J.; Suenobu, T.; Fukuzumi, S. *J. Phys. Chem. A* **2005**, *109*, 9356.
(30) Alloway, B. *Heavy Metals in Soils*; Blackie Academic & Professional: Glasgow, U.K., 1995.
(31) Hassan, A. K.; Pardi, L. A.; Krzystek, J.; Sienkiewicz, A.; Goy, P.; Rohrer, M.; Brunel, L. C. *J. Magn. Reson.* **2000**, *142*, 300.
(32) Neese, F. *J. Chem. Phys.* **2001**, *115*, 11080.
(33) Patchkovskii, S.; Schreckenbach, G. In *Calculation of NMR and EPR Parameters: Theory and Applications*, 1st ed.; Kaupp, M., Buhl, M., Malkin, V. G., Eds.; Wiley VCH: Weinheim, 2004.
(34) Malkina, O. L.; Vaara, J.; Schimmelpfennig, B.; Munzarová, M.; Malkin, V. G.; Kaupp, M. *J. Am. Chem. Soc.* **2000**, *122*, 9206.
(35) van Lenthe, E.; van der Avoird, A.; Wormer, P. E. S. *J. Chem. Phys.* **1997**, *107*, 2488.
(36) van Lenthe, E.; Baerends, E. J.; Snijders, J. G. *J. Chem. Phys.* **1993**, *99*, 4597.
(37) Amsterdam Density Functional (ADF) 2007.01, SCM, Theoretical Chemistry, Vrije Universiteit, Amsterdam, The Netherlands (http://www.scm.com).
(38) Vosko, S. H.; Wilk, L.; Nusair, M. *Can. J. Phys.* **1980**, 1200.
(39) Becke, A. D. *Phys. Rev. A* **1988**, *38*, 3098.
(40) Perdew, J. P. *Phys. Rev. B* **1986**, *33*, 8822. Erratum: Perdew, J. P. *Phys. Rev. B* **1986**, *34*, 7406.
(41) Perdew, J. P.; Chevary, J. A.; Vosko, S. H.; Jackson, K. A.; Pederson, M. R.; Singh, D. J.; Fiolhais, C. *Phys. Rev. B* **1992**, *46*, 6671.
(42) Lee, C.; Yang, W.; Parr, R. G. *Phys. Rev. B* **1988**, *37*, 785.
(43) Eschrig, H.; Servedio, V. D. P. *J. Comput. Chem.* **1999**, *20*, 23.
(44) van Lenthe, E.; Ehlers, A. E.; Baerends, E. J. *J. Chem. Phys.* **1999**, *110*, 8943.
(45) Päch, M.; Macrae, R. M.; Carmichael, I. *J. Am. Chem. Soc.* **2006**, *128*, 6111.
(46) Sasamori, R.; Okaue, Y.; Isobe, T.; Matsuda, Y. *Science* **1994**, *265*, 1691.
(47) Barnard, M. G.; Brown, M. A.; Mabrouk, H. E.; McGarvey, B. R.; Tuck, D. G. *Inorg. Chim. Acta* **2003**, *349*, 142.
(48) Abakumov, G. A.; Cherkasov, V. K.; Piskunov, A. V.; Lado, A. V.; Fukin, G. K.; Abakumova, L. G. *Russ. Chem. Bull., Int. Ed.* **2006**, *55*, 1146.
(49) Yassin, F. H.; Marynick, D. S. *J. Mol. Struct.: THEOCHEM* **2003**, *629*, 223.
(50) Odom, B.; Hanneke, D.; D'Urso, B.; Gabrielse, G. *Phys. Rev. Lett.* **2006**, *97*, 30801.

JP906289D